IMPROVED GEOSPATIAL CONTROL OF MINI-RF BISTATIC OBSERVATIONS. C. Nypaver[1], B. J. Thomson[1], G. W. Patterson[2], S. Bhiravarasu[3], C. Neish[4], L. Jozwiak[2], J.T. Cahill[2]. [1]Department of Earth and Planetary Sciences, University of Tennessee, Knoxville, TN 37996 (cnypaver@vols.utk.edu). [2]Applied Physics Laboratory, Johns Hopkins University, Baltimore, MD 21218. [3]Lunar and Planetary Institute, Houston, TX 77058. [4]Department of Earth Sciences, The University of Western Ontario, London, Ontario, N6A 5B7.

Introduction: The Mini-RF instrument is a hybrid-polarized synthetic aperture radar (SAR) instrument onboard the NASA Lunar Reconnaissance Orbiter (LRO). By original design, the instrument would emit a left-circular polarized signal and receive the horizontal and vertical components of that signal in a monostatic configuration [1, 2]. In Dec. 2010, a malfunction left the Mini-RF antenna unable to transmit signals. The Mini-RF receiver and other instrument subsystems were not affected by the malfunction, so a bistatic architecture was devised [3]. In this configuration, either S-band or X-band radar signals can be transmitted from the Earth-based Arecibo and Goldstone observatories (respectively), reflected off the lunar surface, and then collected by the Mini-RF instrument in lunar orbit [3-5]. The final products of the initial (2012-2015) bistatic campaign were 28 S-band bistatic image swaths while the current, ongoing bistatic campaign has resulted in 4 S-band and 29 X-band observations [3]. The goal of the work presented here is to georectify publicly available non-polar Mini-RF total power and circular polarization ratio (CPR) bistatic images to facilitate comparison with other lunar data sets.

Currently, all bistatic images are publicly available via the Geosciences node of the Planetary Data System (PDS) at University of Washington in St. Louis (http://pds-geosciences.wustl.edu/lro/lro-l-mrflro-2_3_5-bistatic-v2/lromrf_2xxx/data/rdr/), but the geospatial coordinates provided with the reduced data often include substantial areas that do not include image data (**Fig. 1**). The additional geospatial information associated with these images complicates analyses of bistatic angle dependencies and hinders the correlation of Mini-RF data with other lunar datasets. A major goal of the Mini-RF bistatic data collection campaign is to constrain the effects of the observation geometry on various radar properties of the lunar surface [3]. Here we describe a methodology that provides more accurate geospatial information for Mini-RF bistatic radar images. Georectifying the data will simplify analyses of the data and facilitate cross-comparison with other lunar datasets.

Data: Each bistatic image (.img) file available on the PDS possesses an accompanying label (.lbl) ASCII text file which contains all information on the image file and the data collect. The Mini-RF bistatic images are available as 32-bit image files with an average spatial resolution of ~100 m/px; although, this resolution varies somewhat as a function of the bistatic angle and observational parameters. The Mini-RF bistatic data available to the public include level 1 images as reduced data records (RDR) corresponding to all four Stokes parameters and CPR images. Also available are the level 0 experimental data records (EDR) and derived data records (DDR) containing geometric information corresponding to each image (including a latitude and longitude for each pixel in the image). In this work, we use S_1 (total power) and CPR images as they are the most widely utilized for scientific investigations.

Methods: In order to convert the bistatic raster images with a set number of lines and samples to an ArcGIS-compatible format, we used the Integrated System for Imagers and Spectrometers (ISIS3) *pds2isis* tool to convert the bistatic image (.img) files to cube (.cub) files which are ingestible and projectable in ArcGIS 10.6. The size of a single bistatic image cube file ranges from ~1.0–1.6 GB. Image values were then stretched along a custom color ramp based on the individual properties of the image. A common stretch cannot be applied to every S1 image because the unique observation geometries for each bistatic collect can result in large variations in reflected power from the surface.. The images were georeferenced to the LRO WAC global mosaic using manually-identified tie points corresponding to identifiable surface features. The number of tie points used per image varied based on the presence and distribution of surface features, but no fewer than 5 tie points were use to georectify each image. In addition to visible surface features, latitude and image size were controlling factors on the number of tie points used with larger images at higher latitudes requiring more tie points to correct for distortion and offsets. Once georectified, images were assembled into a mosaic using ArcMap. Footprint shapefiles of all images were also created for the true bistatic images using the "*Build footprints*" tool in ArcMap.

Results: The results of this work are global compilations of georectified S-band Mini-RF bistatic S1 and CPR images. We have also produced corresponding shapefiles of image footprints with attribute tables containing all pertinent image information (e.g. orbit number, bandwidth, native resolution, lat/long parameters). An error with the image projection reported in the PDS label files for the Mini-RF bistatic data (equirectangular

vs oblique cylindrical) can produce geospatial inaccuracies of up to 195.6 km from their georectified locations (**Fig. 2**). This inaccuracy refers to the average distance between the given corner coordinates in the PDS label files and the actual corner coordinates on the georectified images. If the bistatic data are projected from the pixel location information in the accompanying DDR file for the image, this error can be mitigated. After georectification, tie points still possess an average geospatial offset of ~4.6 km and a root mean squared error of 0.0948 km^2. Causes of this residual error include the accuracy of timing information from the instrument and spacecraft and the influence of topography on the radar image formation process – i.e., bistatic data currently available in the PDS were processed without accounting for lunar topography.

The entire Mini-RF dataset is being reprocessed to improve the data quality and reduce errors in registration and these reprocessed data will be made available to the public, through the PDS. The issue with the PDS labels highlighted here will be corrected and low-resolution topography (LOLA 4 pixel/°) will be used to form the radar images. In spite of this, it should be noted that, offsets will likely still be present, locally, in areas of significant small-scale variations in lunar surface topography. Further work is required to produce fully controlled mosaics of both S-Band and X-band bistatic images.

References: [1] Raney K. R. et al. (2011) *Proc. IEEE, 99,* 808-823. [2] Nozette S. et al. (2010) *SSR, 150,* 285-302. [3] Patterson, G. W. et al. (2017) *Icarus, 283,* 2-19. [4] Wahl D. E. et al. (2012) Proc. SPIE, 8394. [5] Stickle A. M. et al. (2018) *LPSC 49,* abstract #1585

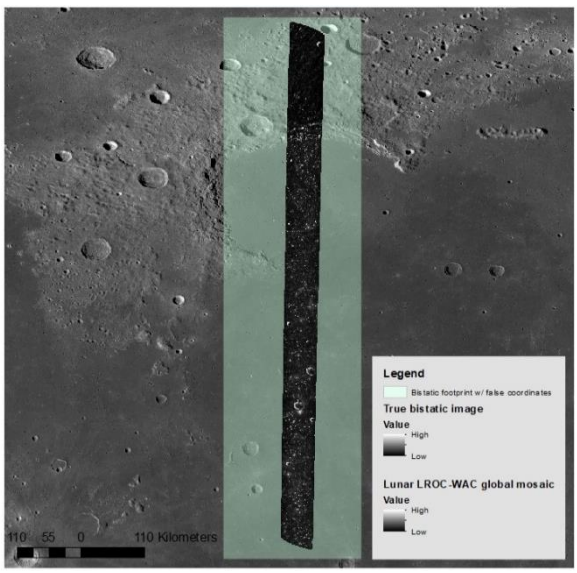

Figure 1: Mini-RF bistatic S_1 image georectified and overlaid onto the LROC WAC global mosaic with the original image footprint (pale green box) as given by PDS coordinates. The PDS corner coordinates are an inaccurate representation of the actual image size in both latitude and longitude.

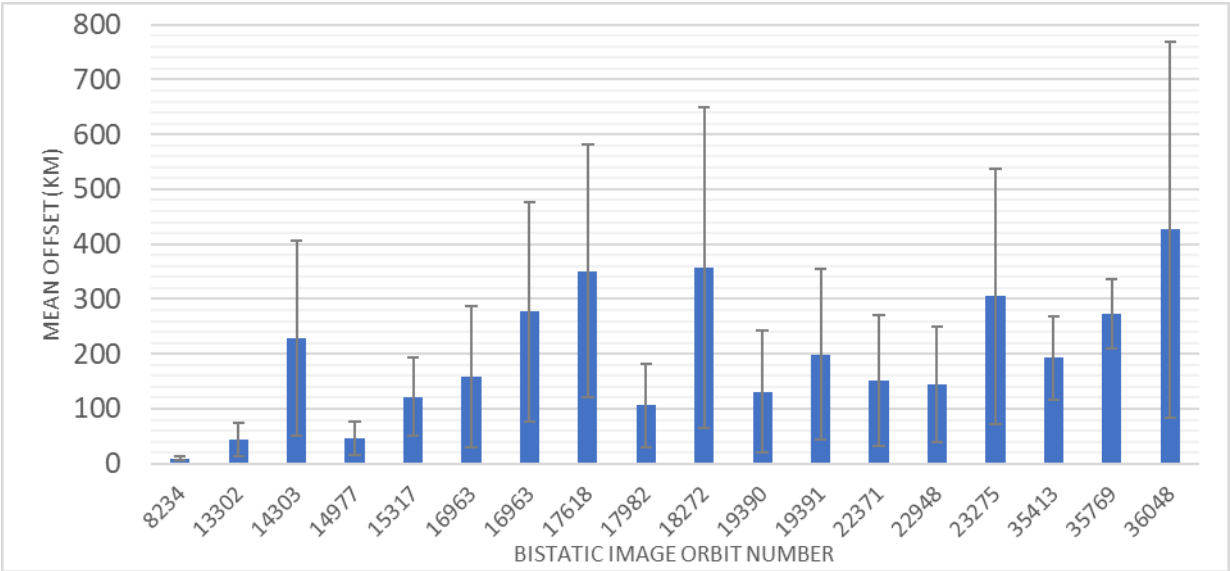

Figure 2: Bar chart showing mean offset from label file corner coordinates for 18 Mini-RF S-band non-polar images.